

ENHANCEMENT OF TITANIUM DIOXIDE (TiO_2) DYE-SENSITIZED SOLAR
CELLS (DSSCs) PERFORMANCE WITH INCORPORATION OF REDUCED
GRAPHENE OXIDE (rGO)

AZMAN BIN TALIB

A thesis submitted in
fulfillment of the requirement for the award of the
Doctor of Philosophy in Electrical Engineering



Faculty of Electrical and Electronic Engineering
Universiti Tun Hussein Onn Malaysia

MARCH 2022

Special dedication to

My lovely wife and precious children;

Norazlina Binti Ahmad

Muhammad Syamil Adha Bin Azman

Nurul Syuhaidah Binti Azman

Nur Syazwani Binti Azman

Muhammad Syafiq Azri Bin Azman

Nurul Ain Syahira Binti Azman



PTTA UTHM
PERPUSTAKAAN TUNKU TUN AMINAH

ACKNOWLEDGEMENT

I would like to express my gratitude to Allah with His permission I can finish my project successfully. Alhamdulillah, His Willingness has made it possible for me as the author to accomplish my research.

Special thanks dedicated to my supervisor Assoc. Prof. Dr. Mohd. Khairul Bin Ahmad for guiding this research at every stage with clarity, spending much time to discuss and help with this research, and that priceless gift of getting done by sharing his valuable ideas as well as his knowledge. Also thank you so much to my co-supervisor Assoc. Prof. Dr. Fariza Binti Mohamad for her guidance and discussion that really helped me in completing this research.

I am very greatly indebted to the Microelectronics and Nanotechnology - Shamsudin Research Centre (MiNT-SRC) family members and Faculty of Electrical and Electronic Engineering, Universiti Tun Hussein Onn Malaysia for providing excellent lab facilities that make this work possible. Not forgotten to the expert in-charged person especially Miss Faezahana Binti Mohkhter, Mr. Ahmad Nasrul Bin Mohamed and Mr. Mohd. Azwadi Bin Omar that really helped my research runs smoothly.

I also want to show my gratefulness to the Ministry of High Education on the financial support through the scholarship and privileges provided in Hadiah Latihan Persekutuan (HLP) programme in furthering my study in the doctorate level.

To my wife and lovely children, thank you for your love, time, supporting and understanding throughout the duration on completing this research. Also thanks to my colleagues for their support and encouragement me to make this research successful.

ABSTRACT

The purpose of this thesis is to investigate the structural, optical and electrical properties of titanium dioxide (TiO_2) dye-sensitized solar cells (DSSCs) with the incorporation of reduced graphene oxide (rGO). In this experiment, rGO from electrochemical exfoliation, was deposited onto few fluorine-doped tin-oxide (FTO) substrat through spray pyrolysis deposition (SPD) method with different rGO volumes. Then, all the fabricated FTOs went through rutile-phase TiO_2 (r- TiO_2) with hydrothermal synthesis. From DSSCs analysis, 0.50 mL of rGO volume exhibited the best photovoltaic (PV) performance with the efficiency of 2.61% and open-circuit voltage of 0.70 V. The successful synthesis of rGO, incorporated with TiO_2 was confirmed using Raman spectroscopy. The analysis of the samples was done using X-ray diffraction, field emission scanning electron microscopy, ultraviolet-visible spectrophotometry, and incident photon-to-carrier conversion efficiency spectra. Then, another rGO which was produced through Hummers method, was incorporated into anatase-phase TiO_2 (a- TiO_2) as nanocomposite (NC) mixture. After that, through SPD method, the NC mixture was deposited onto few FTOs. The a- TiO_2 was produced by adding TKC-302 into TiO_2 P25 powder. The NC mixture samples significantly contributed towards the improvement of efficiency, when compared with samples without rGO. When 2 mL of rGO was added into a- TiO_2 , PV performance achieved the highest efficiency of 3.15% and current density of 5.98 mA/cm^2 . Finally, the combination of rGO and a- TiO_2 NC mixture, was overlayered onto r- TiO_2 . The 2 mL of rGO/a- TiO_2 NC mixture which was deposited through SPD onto r- TiO_2 , exhibited the best PV performance with the highest efficiency of 5.72% and the current density of 10.37 mA/cm^2 . The rGO acted as an important material, to maximise the photogenerated electrons of photo-induced charge carriers. The photogenerated electrons from dyes transferred through r- TiO_2 , effectively traveled out to the circuit load, which underwent recombination with holes in the solar cells with enhancement of rGO functions.

ABSTRAK

Kandungan tesis ini adalah bagi menyiasat ciri-ciri struktur, optikal dan elektrikal bagi titanium dioksida (TiO_2) *dye-sensitized solar cells* (DSSCs) dengan gabungan *reduced graphene oxide* (*rGO*). Dalam eksperimen ini, *rGO* hasil dari pengelupasan elektrokimia, disemburkan ke atas beberapa keping *fluorine-doped tin-oxide* (*FTO*) dengan kaedah semburan dengan isipadu *rGO* yang berlainan. Kemudian, kesemua *FTO* tersebut akan melalui proses sintesis hidrotermal fasa-rutil titanium dioksida (*r-TiO₂*). Dari analisis *DSSCs*, sampel *rGO* dengan 0.50 mL menunjukkan prestasi fotovoltaik (*PV*) terbaik dengan kecekapan 2.61% dan voltan litar-terbuka 0.70 V. Kejayaan mensintesis *rGO*, dan digabungkan bersama dengan *TiO₂* ditentusahkan menggunakan spektroskopi *Raman*. Analisis ke atas sampel pula menggunakan difraksi sinar-X (*XRD*), mikroskop elektron pengimbas pelepasan medan (*FE-SEM*), sinar ultraungu (*UV-Vis*) spektrofotometri, dan spektrum kecekapan penukaran foton ke pembawa kejadian (*IPCE*). Kemudian, *rGO* lain yang disintesis melalui kaedah *Hummers*, digabungkan ke dalam larutan fasa-anates *TiO₂* (*a-TiO₂*) sebagai campuran nanokomposit (*NC*), dan disemburkan ke atas beberapa keping *FTO*. Larutan *a-TiO₂* tersebut dihasilkan daripada serbuk *TiO₂* P25 yang dicampurkan dengan TKC-302. Campuran *NC* tersebut memberikan kesan peningkatan pada kecekapan *PV* sel, berbanding tanpa menggunakan *rGO*. Isipadu 2 mL *rGO* yang ditambahkan kepada *a-TiO₂*, menghasilkan kecekapan PV tertinggi iaitu 3.15% dan ketumpatan arus 5.98 mA/cm². Dan akhir sekali, kombinasi campuran *rGO* dan *a-TiO₂ NC*, yang disembur ke atas struktur *r-TiO₂ NS*. Isipadu 2 mL campuran *rGO/a-TiO₂ NC*, disemburkan ke atas struktur *r-TiO₂*, menghasilkan prestasi fotovoltaik terbaik dengan kecekapan penukaran tertinggi 5.72% dan ketumpatan arus 10.37 mA/cm². *rGO* bertindak sebagai bahan gabungan ke dalam *a-TiO₂*, memaksimumkan bilangan elektron pembawa cas. Membolehkan elektron dari *dye* dipindahkan melalui *r-TiO₂ NS*, bergerak secara efektif ke beban, dengan menghalang penggabungan semula dengan lubang di sel suria dengan meningkatnya fungsi *rGO*.

CONTENTS

| | |
|--|--------------|
| TITLE | i |
| DECLARATION | ii |
| DEDICATION | iii |
| ACKNOWLEDGEMENT | iv |
| ABSTRACT | v |
| ABSTRAK | vi |
| LIST OF TABLES | xii |
| LIST OF FIGURES | xiv |
| LIST OF SYMBOLS AND ABBREVIATIONS | xx |
| LIST OF APPENDICES | xxiii |
| CHAPTER 1 INTRODUCTION | 1 |
| 1.1 Introduction | 1 |
| 1.2 Research background | 3 |
| 1.3 Problem statement | 5 |
| 1.4 Objectives of the research | 7 |
| 1.5 Scope of the research | 7 |
| 1.6 Contribution of the research | 8 |
| 1.7 Thesis outline | 8 |

| | |
|---|-----------|
| CHAPTER 2 LITERATURE REVIEW | 10 |
| 2.1 Introduction | 10 |
| 2.2 Fluorine-doped tin oxide glass substrate | 10 |
| 2.3 Titanium dioxide | 12 |
| 2.4 Hydrothermal synthesis | 14 |
| 2.5 Spray Pyrolysis Deposition | 16 |
| 2.6 Dyes | 17 |
| 2.7 Electrolyte | 20 |
| 2.8 Counter electrode | 21 |
| 2.9 Dye-sensitized solar cells (DSSCs) | 22 |
| 2.10 Reduced graphene oxide (rGO) | 24 |
| 2.11 Research gap | 26 |
| CHAPTER 3 METHODOLOGY | 28 |
| 3.1 Introduction | 28 |
| 3.1.1 FTO substrate cleaning | 28 |
| 3.1.2 The common fabrication process of r-TiO ₂ NRs/NFs thin film on FTO substrate using hydrothermal synthesis method | 30 |
| 3.1.3 Sample characterization | 32 |
| 3.1.4 Solar simulator measurement | 33 |
| 3.1.5 Properties characterization | 34 |
| 3.2 Hydrothermal synthesis of r-TiO ₂ NRs/NFs with various TBOT precursor volume | 35 |
| 3.2.1 Preparation for the hydrothermal synthesis | 35 |
| 3.3 Hydrothermal synthesis of r-TiO ₂ NRs/NFs with various reaction time | 37 |
| 3.3.1 Preparation for the hydrothermal synthesis | 38 |

| | |
|---|----|
| 3.3.2 Solar simulator measurement | 39 |
| 3.4 Hydrothermal synthesis of r-TiO ₂ NS direct growth on FTO/rGO thin film | 40 |
| 3.4.1 Preparation of rGO by using electrochemical exfoliation method and reducing process | 40 |
| 3.4.2 Deposition of rGO layer onto FTO/rGO thin film | 42 |
| 3.4.3 Preparation for the hydrothermal synthesis | 43 |
| 3.4.4 Solar simulator measurement | 44 |
| 3.5 Effect of various rGO/a-TiO ₂ NC mixture volume, SPD onto FTO substrate | 45 |
| 3.5.1 Preparation of rGO via improved Hummers method and reducing process | 46 |
| 3.5.2 Preparation of a-TiO ₂ NPs solution | 47 |
| 3.5.3 Preparation of NC mixture of rGO incorporated into a-TiO ₂ NPs solution | 47 |
| 3.5.4 Deposition of pure a-TiO ₂ and rGO/a-TiO ₂ NC mixture, SPD onto FTO substrate | 47 |
| 3.5.5 Solar simulator measurement | 49 |
| 3.6 Effect of deposition various a-TiO ₂ NPs volume, overlaid onto r-TiO ₂ NS | 49 |
| 3.6.1 Preparation for the hydrothermal synthesis | 50 |
| 3.6.2 Preparation of a-TiO ₂ NPs solution | 50 |
| 3.6.3 Deposition of various a-TiO ₂ NPs volume, overlaid onto r-TiO ₂ NS | 51 |
| 3.6.4 Solar simulator measurement | 52 |
| 3.7 Effect of various rGO volume incorporate into a-TiO ₂ NPs, overlaid onto r-TiO ₂ NS | 53 |
| 3.7.1 Preparation for hydrothermal synthesis | 54 |
| 3.7.2 Preparation of rGO | 54 |

| | |
|---|-----------|
| 3.7.3 Preparation of a-TiO ₂ NPs solution | 54 |
| 3.7.4 Preparation of rGO incorporated into a-TiO ₂ NPs solution | 54 |
| 3.7.5 Deposition of rGO/a-TiO ₂ NC mixture onto r-TiO ₂ NS | 54 |
| 3.7.6 Solar simulator measurement | 56 |
| CHAPTER 4 RESULTS AND DISCUSSION | 58 |
| 4.1 Introduction | 58 |
| 4.2 Hydrothermal synthesis of r-TiO ₂ NRs/NFs with various TBOT precursor volume | 58 |
| 4.2.1 Structural analysis | 58 |
| 4.2.2 Surface morphology | 61 |
| 4.2.3 Optical properties | 64 |
| 4.2.4 Electrical properties | 67 |
| 4.3 Hydrothermal synthesis of r-TiO ₂ NRs/NFs with various reaction time | 68 |
| 4.3.1 Structural analysis | 68 |
| 4.3.2 Surface morphology | 70 |
| 4.3.3 Optical properties | 76 |
| 4.3.4 Electrical properties | 78 |
| 4.4 Hydrothermal synthesis of r-TiO ₂ NS direct growth on FTO/rGO thin film | 82 |
| 4.4.1 Structural analysis | 82 |
| 4.4.2 Surface morphology | 84 |
| 4.4.3 Optical properties | 86 |
| 4.4.4 Electrical properties | 87 |
| 4.5 Effect of various rGO/a-TiO ₂ NC mixture volume, SPD onto FTO substrates | 90 |
| 4.5.1 Structural analysis | 90 |
| 4.5.2 Surface morphology | 97 |

| | |
|---|------------|
| 4.5.3 Optical properties | 100 |
| 4.5.4 Electrical properties | 103 |
| 4.6 Effect of deposition various a-TiO ₂ NPs volume, overlayered onto r-TiO ₂ NS thin film | 107 |
| 4.6.1 Structural analysis | 107 |
| 4.6.2 Surface morphology | 109 |
| 4.6.3 Optical properties | 110 |
| 4.6.4 Electrical properties | 111 |
| 4.7 Effect of various rGO volume incorporate into a-TiO ₂ NPs, overlayered onto r-TiO ₂ NS | 114 |
| 4.7.1 Structural analysis | 114 |
| 4.7.2 Surface morphology | 117 |
| 4.7.3 Optical properties | 118 |
| 4.7.4 Electrical properties | 119 |
| CHAPTER 5 CONCLUSION AND RECOMMENDATIONS | 122 |
| 5.1 Introduction | 122 |
| 5.2 Conclusion | 122 |
| 5.3 Recommendation | 124 |
| REFERENCES | 125 |
| APPENDICES | 146 |

LIST OF TABLES

| | | |
|-----|--|----|
| 2.1 | The efficiency of morphology combination in solar cells fabrication. | 16 |
| 2.2 | I-V measurement of DSSCs based on various types of natural dyes [102]. | 20 |
| 2.3 | The DSSCs efficiency of TiO ₂ phases with rGO incorporation fabrication. | 27 |
| 3.1 | Hydrothermal synthesis with various TBOT precursor volume. | 36 |
| 3.2 | The label of the prepared samples under various TBOT volume. | 36 |
| 3.3 | Hydrothermal synthesis with various reaction time. | 38 |
| 3.4 | Label of the prepared samples at various reaction time. | 38 |
| 3.5 | Label of r-TiO ₂ NS samples direct growth on FTO/rGO substrate. | 43 |
| 3.6 | Label of pure a-TiO ₂ and rGO/a-TiO ₂ NC mixture samples on the FTO substrate. | 48 |
| 3.7 | Label of a-TiO ₂ NPs volume samples, overlaid onto r-TiO ₂ NS. | 52 |
| 3.8 | Label of rGO/a-TiO ₂ NC mixture samples onto r-TiO ₂ NS. | 55 |
| 4.1 | Predominant crystallite size variant under different TBOT volume. | 61 |
| 4.2 | The size of r-TiO ₂ NRs/NFs growth using various TBOT volume. | 64 |
| 4.3 | Values of the energy bandgap of samples (a) TB3 (b) TB4 (c) TB5 and (d) TB6. | 66 |
| 4.4 | Electrical properties of samples for various TBOT volume. | 67 |
| 4.5 | Full-width Half-Maximum and crystallite size of sample fabricated with different reaction time. | 70 |
| 4.6 | The size of TiO ₂ growth under various hydrothermal reaction time. | 71 |
| 4.7 | The EDX data for samples prepared at various reaction time. | 76 |
| 4.8 | Values of the energy bandgap of RT5, RT10, RT15, RT20 and RT25 prepared samples. | 77 |

| | | |
|------|--|-----|
| 4.9 | Electrical properties of prepared samples at various reaction time. | 79 |
| 4.10 | Photovoltaic parameters of DSSCs with different TiO ₂ reaction time. | 80 |
| 4.11 | Structural parameters calculated from XRD patterns for r-TiO ₂ NS direct growth on FTO/rGO. | 84 |
| 4.12 | EDX data for prepared samples at different rGO volume for r-TiO ₂ NS direct growth on FTO/rGO. | 86 |
| 4.13 | Photovoltaic parameters of DSSCs with different rGO volume of r-TiO ₂ NS direct growth on FTO/rGO. | 88 |
| 4.14 | Values of the energy bandgap of various rGO/a-TiO ₂ NC mixture. | 103 |
| 4.15 | Photovoltaic parameters DSSCs various rGO/a-TiO ₂ NC mixture volume. | 104 |
| 4.16 | Photovoltaic parameters DSSCs of highest efficiency sample without rGO, and with rGO incorporation. | 107 |
| 4.17 | Photovoltaic parameters of DSSCs of various a-TiO ₂ NPs volume overlayed onto r-TiO ₂ NS thin film. | 111 |
| 4.18 | Photovoltaic parameters of DSSCs of various rGO volume incorporated into a-TiO ₂ NPs, overlayed onto r-TiO ₂ NS. | 119 |

LIST OF FIGURES

| | |
|---|----|
| 1.1 Generations of solar cells technology [5]. | 2 |
| 2.1 Ball and stick of the structure of SnO ₂ [48]. | 11 |
| 2.2 The schematic drawing of the SnO ₂ film at an early stage formed by the SPD process [51]. | 12 |
| 2.3 Unit cells of the TiO ₂ modifications rutile, brookite and anatase (from left to right) [56]. | 13 |
| 2.4 Spray pyrolysis deposition method [90]. | 17 |
| 2.5 Molecular structure of several metal-complex dye with efficiency [97]. | 18 |
| 2.6 Working mechanism of metal-free organic dye. Do and Acc are denoting donor and acceptor, respectively [98]. | 19 |
| 2.7 Structure and the viscosity of several ionic liquids [104]. | 21 |
| 2.8 Layers of DSSCs components [115]. | 23 |
| 2.9 A schematic diagram of a DSSCs showing the principles of operation [71]. | 24 |
| 2.1 Fullerene (0D), nanotube (1D), graphene (2D), and graphite (3D) (from left to right) [120], [121]. | 26 |
| 2.11 The derivatives of graphene. | 26 |
| 3.1 Process for experiments synthesis and characterization. | 29 |
| 3.2 FTO substrate cleaning procedure. | 30 |
| 3.3 Teflon-lined stainless steel autoclave. | 31 |
| 3.4 Illustration of the FTO substrate leans against the container wall. | 32 |
| 3.5 Photoanode immersed in N719 dye. | 33 |
| 3.6 Pt CE and photoanode clamped for efficiency measurement under solar simulator tester. | 34 |
| 3.7 Chart of various TBOT precursor volume. | 35 |

| | | |
|------|--|----|
| 3.8 | Hydrothermal synthesis with various TBOT precursor volume. | 37 |
| 3.9 | Chart of various reaction time. | 37 |
| 3.1 | Hydrothermal synthesis with various reaction time. | 39 |
| 3.11 | Illustration of r-TiO ₂ NRs/NFs test circuit measurement. | 39 |
| 3.12 | Chart for hydrothermal synthesis of r-TiO ₂ NS direct growth on FTO/rGO substrate. | 40 |
| 3.13 | Electrochemical exfoliation process. | 41 |
| 3.14 | GO reducing process to rGO by hydrazine hydrate. | 42 |
| 3.15 | Hydrothermal synthesis of r-TiO ₂ NS direct growth on FTO/rGO substrate. | 44 |
| 3.16 | Illustration of r-TiO ₂ NS direct growth on FTO/rGO test circuit measurement. | 45 |
| 3.17 | Chart of various rGO/a-TiO ₂ NC mixture volume, onto the FTO substrate. | 46 |
| 3.18 | Various rGO/a-TiO ₂ NC mixture volume, SPD onto FTO substrate. | 48 |
| 3.19 | Illustration of rGO/a-TiO ₂ NC test circuit measurement. | 49 |
| 3.2 | Chart of various a-TiO ₂ NPs volume, overlaid onto r-TiO ₂ NS. | 50 |
| 3.21 | Various a-TiO ₂ NPs volume, overlaid onto r-TiO ₂ NS. | 51 |
| 3.22 | Illustration of a-TiO ₂ NPs overlaid onto r-TiO ₂ NS test circuit measurement. | 52 |
| 3.23 | Chart of various rGO volume incorporated into a-TiO ₂ NPs, overlaid on r-TiO ₂ NS. | 53 |
| 3.24 | Various rGO/a-TiO ₂ NC mixture volume, overlaid onto r-TiO ₂ NS. | 55 |
| 3.25 | Illustration of rGO/a-TiO ₂ NC overlaid onto r-TiO ₂ NS solar simulator circuit. | 56 |
| 3.26 | Schematic diagram of rGO/a-TiO ₂ NC overlaid onto r-TiO ₂ NS DSSCs. | 57 |
| 4.1 | XRD peak patterns of r-TiO ₂ NRs/NFs prepared using (a) TB3 (b) TB4 (c) TB5 and (d) TB6 of TBOT volume. | 59 |
| 4.2 | FE-SEM images of TB3 under (a) 5,000x (b) 50,000x magnification (c) cross-section view, and (d) EDX spectrum. | 62 |

| | | |
|------|---|----|
| 4.3 | FE-SEM images of TB4 under (a) 5,000x (b) 50,000x magnification (c) cross-section view, and (d) EDX spectrum. | 63 |
| 4.4 | FE-SEM images of TB5 under (a) 5,000x (b) 30,000x magnification (c) cross-section view, and (d) EDX spectrum. | 63 |
| 4.5 | FE-SEM images of TB6 under (a) 5,000x (b) 50,000x magnification (c) cross-section view, and (d) EDX spectrum. | 64 |
| 4.6 | UV-Vis spectra of r-TiO ₂ samples (a) TB3 (b) TB4 (c) TB5 and (d) TB6. | 65 |
| 4.7 | Bandgap estimation of (a) TB3, (b) TB4, (c) TB5, and (d) TB6 prepared samples. | 66 |
| 4.8 | XRD patterns of the as-synthesis samples (a) RT5 (b) RT10 (c) RT15 (d) RT20 and (e) RT25 at 150 °C, respectively. | 69 |
| 4.9 | FE-SEM images of r-TiO ₂ NRs/NFs synthesis at 5 hours under (a) 5,000x (b) 30,000x magnification (c) cross-section view, and (d) EDX spectrum. | 73 |
| 4.10 | FE-SEM images of r-TiO ₂ NRs/NFs synthesis at 10 hours under (a) 5,000x (b) 30,000x magnifications (c) cross-section view, and (d) EDX spectrum. | 73 |
| 4.11 | FE-SEM images of r-TiO ₂ NRs/NFs synthesis at 15 hours under (a) 5,000x (b) 30,000x magnification (c) cross-section view, and (d) EDX spectrum. | 74 |
| 4.12 | FE-SEM images of r-TiO ₂ NRs/NFs synthesis at 20 hours under (a) 5,000x (b) 30,000x magnification (c) cross-section view, and (d) EDX spectrum. | 74 |
| 4.13 | FE-SEM images of r-TiO ₂ NRs/NFs synthesis at 25 hours under (a) 5,000x (b) 30,000x magnification (c) cross-section view, and (d) EDX spectrum. | 75 |
| 4.14 | UV-Vis spectra of (a) RT5 (b) RT10 (c) RT15 (d) RT20 and (e) RT25 of r-TiO ₂ thin film. | 76 |
| 4.15 | Bandgap estimation of (a) RT5, (b) RT10, RT15, RT20 and RT25 prepared samples. | 78 |
| 4.16 | J-V characteristics of the DSSCs made with TiO ₂ photoanodes of different reaction time. | 80 |

| | | |
|------|--|----|
| 4.17 | The IPCE spectra of DSSCs made with TiO ₂ thin film of different reaction time. | 81 |
| 4.18 | Raman spectra of rGO. | 82 |
| 4.19 | XRD patterns of FTO/rGO/TiO ₂ thin film synthesis (a) bare FTO substrate (b) FT_Ref (c) FRT_0.25 (d) FRT_0.50 (e) FRT_0.75 and (f) FRT_1.00. | 83 |
| 4.20 | FE-SEM pictures of the samples prepared (a) FRT_0.25 (b) FRT_0.50 (c) FRT_0.75 and (d) FRT_1.00 (e) FT_Ref | 85 |
| 4.21 | UV-Vis spectra of the (a) FT_Ref (b) FRT_0.25 (c) FRT_0.50 (d) FRT_0.75 and (e) FRT_1.00. | 87 |
| 4.22 | J-V characteristics of the DSSCs (a) FT_Ref (b) FRT_0.25 (c) FRT_0.50 (d) FRT_0.75 and (e) FRT_1.00. | 88 |
| 4.23 | The IPCE spectra of DSSCs (a) FRT_0.25 (b) FRT_0.50 (c) FRT_0.75 (d) FRT_1.00 and (e) FT_Ref. | 90 |
| 4.24 | Raman spectra of (a) a-T_1, (b) a-T_2, (c) a-T_3 and (d) a-T_4. | 91 |
| 4.25 | Raman intensity of the first Eg(1) mode of (a) a-T_1, (b) a-T_2, (c) a-T_3, and (d) a-T_4. | 92 |
| 4.26 | Raman spectra of Raman shift (100-800 cm ⁻¹) (a) R/a-T_1, (b) R/a-T_2, (c) R/a-T_3, and (d) R/a-T_4. | 93 |
| 4.27 | Raman spectra of Raman shift (1000-3000 cm ⁻¹) (a) R/a-T_1, (b) R/a-T_2, (c) R/a-T_3, and (d) R/a-T_4. | 94 |
| 4.28 | Raman intensity of the first Eg mode of (a) R/a-T_1, (b) R/a-T_2, (c) R/a-T_3, and (d) R/a-T_4. | 95 |
| 4.29 | ID/IG ratio and IG/I2D ratio of a-T and R/a-T samples respectively versus volume spray. | 96 |
| 4.30 | XRD patterns of (a) a-T_1, (b) a-T_2, (c) a-T_3, (d) a-T_4, (e) R/a-T_1, (f) R/a-T_2, (g) R/a-T_3, and (h) R/a-T_4. | 97 |
| 4.31 | FE-SEM images of cross-section view of (a) a-T_1, (b) a-T_2, (e) R/a-T_1, and (f) R/a-T_2 under 15,000x magnification, (c) a-T_3 and (g) R/a-T_3 under 10,000x magnification, (d) a-T_4, and (h) R/a-T_4 under 7,000x magnification. | 99 |

| | | |
|------|---|-----|
| 4.32 | UV-Vis spectra of the N719-loaded (a) a-T_1, (b) a-T_2, (c) a-T_3, (d) a-T_4, (e) R/a-T_1, (f) R/a-T_2, (g) R/a-T_3, and (h) R/a-T_4. | 100 |
| 4.33 | Bandgap estimation of the N719-loaded (a) a-T_1, (b) a-T_2, (c) a-T_3, (d) a-T_4, (e) R/a-T_1, (f) R/a-T_2, (g) R/a-T_3, and (h) R/a-T_4. | 102 |
| 4.34 | J-V characteristics of the DSSCs (a) a-T_1, (b) a-T_2, (c) a-T_3, (d) a-T_4 (e) R/a-T_1, (f) R/a-T_2, (g) R/a-T_3 and (h) R/a-T_4. | 103 |
| 4.35 | The IPCE spectra of DSSCs (a) a-T_1, (b) a-T_2, (c) a-T_3, (d) a-T_4, (e) R/a-T_1, (f) R/a-T_2, (g) R/a-T_3, and (h) R/a-T_4. | 106 |
| 4.36 | J-V characteristics of highest efficiency sample without rGO (a) a-T_4, and with rGO incorporation (b) R/a-T_4. | 106 |
| 4.37 | XRD patterns of thin film synthesis (a) a-r-T_4, (b) a-r-T_3, (c) a-r-T_2, (d) a-r-T_1, (e) FT_Ref and (f) a-TiO ₂ NPs on FTO. | 108 |
| 4.38 | FE-SEM images of cross-section view of (a) a-r-T_1, (b) a-r-T_2, (c) a-r-T_3, and (d) a-r-T_4 under 3,000x magnifications. | 109 |
| 4.39 | UV-Vis spectra of the N719-loaded (a) a-r-T_4, (b) a-r-T_3, (c) a-r-T_2, (d) a-r-T_1 and (e) FT_Ref. | 110 |
| 4.40 | J-V characteristics of the DSSCs (a) a-r-T_1, (b) a-r-T_2, (c) a-r-T_3, (d) a-r-T_4 and (e) FT_Ref. | 112 |
| 4.41 | The IPCE spectra of DSSCs (a) a-r-T_1, (b) a-r-T_2, (c) a-r-T_3, (d) a-r-T_4 and (e) FT_Ref. | 113 |
| 4.42 | Raman spectra of (a) RT_1, (b) RT_2, (c) RT_3, (d) RT_4 and (e) FT_Ref. | 114 |
| 4.43 | XRD patterns of thin film synthesis (a) RT_4, (b) RT_3, (c) RT_2, (d) RT_1 and (e) FT_Ref. | 116 |
| 4.44 | FE-SEM images of cross-section view of (a) RT_1, (b) RT_2, (c) RT_3, and (d) RT_4 under 3,300x magnifications. | 117 |
| 4.45 | UV-Vis spectra of the N719-loaded (a) RT_1, (b) RT_2, (c) RT_3, (d) RT_4 and (e) FT_Ref. | 118 |
| 4.46 | J-V characteristics of the DSSCs (a) RT_1, (b) RT_2, (c) RT_3, (d) RT_4 and (e) FT_Ref. | 120 |

- 4.47 The IPCE spectra of DSSCs (a) RT_4, (b) RT_3, (c) RT_2, 121
(d) RT_1 and (e) FT_Ref.



LIST OF SYMBOLS AND ABBREVIATIONS

| | | |
|--------------------|---|----------------------------------|
| θ | - | angle |
| λ | - | wavelength |
| $^{\circ}\text{C}$ | - | degree celsius |
| β | - | Full Width Half Maximum (FWHM) |
| l | - | length |
| w | - | width |
| t | - | thickness of the films |
| h | - | hour |
| η | - | efficiency |
| D | - | crystallite size |
| K | - | Scherrer constant |
| E | - | applied potential (V) |
| i | - | current response (A) |
| v | - | scan rate (mV.s^{-1}) |
| ρ | - | resistivity of the films |
| R_s | - | sheet resistance |
| α | - | absorption coefficient |
| E_g | - | energy bandgap |
| R | - | resistivity |
| $\hbar v$ | - | photon energy |
| $0D$ | - | zero-dimensional |
| $1D$ | - | one-dimensional |
| $2D$ | - | two-dimensional |
| $3D$ | - | three-dimensional |
| μm | - | micrometre |
| Abs | - | absorbance |

| | | |
|------------------------|---|---|
| <i>CE</i> | - | counter electrode |
| <i>Cl</i> | - | chloride |
| <i>CO</i> ₂ | - | carbon dioxide |
| <i>C</i> | - | carbon |
| <i>DSSCs</i> | - | dye-sensitized solar cells |
| <i>FE-SEM</i> | - | Field Emission – Scanning Electron Microscope |
| <i>FF</i> | - | fill factor |
| <i>FTO</i> | - | fluorine doped tin-oxide |
| <i>FWHM</i> | - | full width half maximum |
| <i>GW</i> | - | giga watt |
| <i>H</i> | - | hydrogen |
| <i>HCl</i> | - | hydrochloric acid |
| <i>IR</i> | - | infrared |
| <i>I</i> | - | current (A) |
| <i>V</i> | - | voltage (V) |
| <i>ITO</i> | - | indium doped tin-oxide |
| <i>J</i> _{sc} | - | short-circuit current density (mA/cm ²) |
| <i>MΩ</i> | - | mega ohm |
| <i>MW</i> | - | mega watt |
| <i>Na</i> | - | sodium |
| <i>NC</i> | - | nanocomposite |
| <i>NFs</i> | - | nanoflowers |
| <i>nm</i> | - | nanometre |
| <i>NPs</i> | - | nano particles |
| <i>NRs</i> | - | nanorods |
| <i>O</i> | - | oxygen |
| <i>OH</i> | - | hydroxide |
| <i>p</i> | - | positive |
| <i>Pt</i> | - | platinum |
| <i>PCE</i> | - | power energy conversion efficiency |
| <i>PV</i> | - | photovoltaic |
| <i>RE</i> | - | renewable energy |
| <i>RMS</i> | - | root mean square |

| | | |
|--|---|--|
| <i>Si</i> | - | silicone |
| <i>SnO₂</i> | - | tin oxide |
| <i>Sn</i> | - | tin |
| <i>T</i> | - | transmittance |
| <i>TBOT</i> | - | titanium butoxide |
| <i>TCO</i> | - | transparent conducting oxide |
| <i>Ti</i> | - | titanium |
| <i>TiO₂</i> | - | titanium dioxide |
| <i>a-TiO₂</i> | - | anatase-phase of titanium dioxide |
| <i>r-TiO₂</i> | - | rutile-phase of titanium dioxide |
| <i>DI</i> | - | de-ionized |
| <i>EDX</i> | - | energy dispersive x-ray |
| <i>CVD</i> | - | chemical vapour deposition |
| <i>EIS</i> | - | electrochemical impedance spectroscopy |
| <i>GO</i> | - | graphene oxide |
| <i>rGO</i> | - | reduced graphene oxide |
| <i>H₂O₂</i> | - | hydrogen peroxide |
| <i>H₂SO₄</i> | - | sulphuric acid |
| <i>H₃PO₄</i> | - | phosphoric acid |
| <i>KMnO₄</i> | - | potassium permanganate |
| <i>mL</i> | - | millilitre |
| <i>SPD</i> | - | spray pyrolysis deposition |
| <i>SDS</i> | - | sodium dodecyl sulfate |
| <i>TBP</i> | - | 4- <i>tert</i> -butylpyridine |
| <i>UV</i> | - | ultraviolet |
| <i>UV-Vis</i> | - | ultraviolet-visible |
| <i>V_{oc}</i> | - | open-circuit voltage (V) |
| <i>XRD</i> | - | x-ray diffraction |
| <i>atm</i> | - | atmosphere |
| <i>RF</i> | - | radio frequency |
| <i>Ru</i> | - | ruthenium |
| <i>I⁻/I₃⁻</i> | - | iodide/triiodide |
| <i>ZnO</i> | - | zinc oxide |

LIST OF APPENDICES

| APPENDIX | TITLE | PAGE |
|-----------------|----------------------|-------------|
| A | List of Publications | 146 |
| B | VITA | 149 |



PTTA UTHM
PERPUSTAKAAN TUNKU TUN AMINAH

CHAPTER 1

INTRODUCTION

1.1 Introduction

The energy produced by fossil fuels has become today's primary driver in the growth of civilization. The produced energy will affect industrial and agricultural development of any country. Therefore, the survival of a country relies on the continuous conservation of resources. The high availability of fossil fuels will add to a nation's economic richness and materials standards. The intensive use of fossil fuels could affects the atmosphere and ecology [1]. With the demand for electricity, several countries are searching for environmentally sustainable, green and non-conventional alternatives [2]. Solar power is one of the possible forms of green electricity. Solar energy becomes an effective energy source and a critical energy resource since it is one of the renewables that may be utilized when other supplies including fossil fuels have been exhausted. With the high promotion of solar panels, there have been developments in the number of innovations that utilize solar cells in solar energy science.

The so-called solar cells is a photovoltaic structure used primarily to transform solar radiation to electricity dependent on sunlight photosynthesis. The solar cells is an efficient and useful system because of its electricity production capabilities that have been explored extensively in a variety of recent reports [3], [4]. As summarized in Figure 1.1, the solar cells are categorized into three generations based on the time period in which it was discovered. Initially, thin silicon wafer was used to manufacture most of the solar cells. They are also known as the first-generation solar cells. Then, the third generation solar cells are the most advanced cells. They have multijunction

and hot carrier cells, consist of nanomaterials and polymers and are able to exhibit the optimum features compared to earlier generations. They are more efficient, less expensive and adopt the up-conversion, down-conversion, and solar thermal technologies [5].

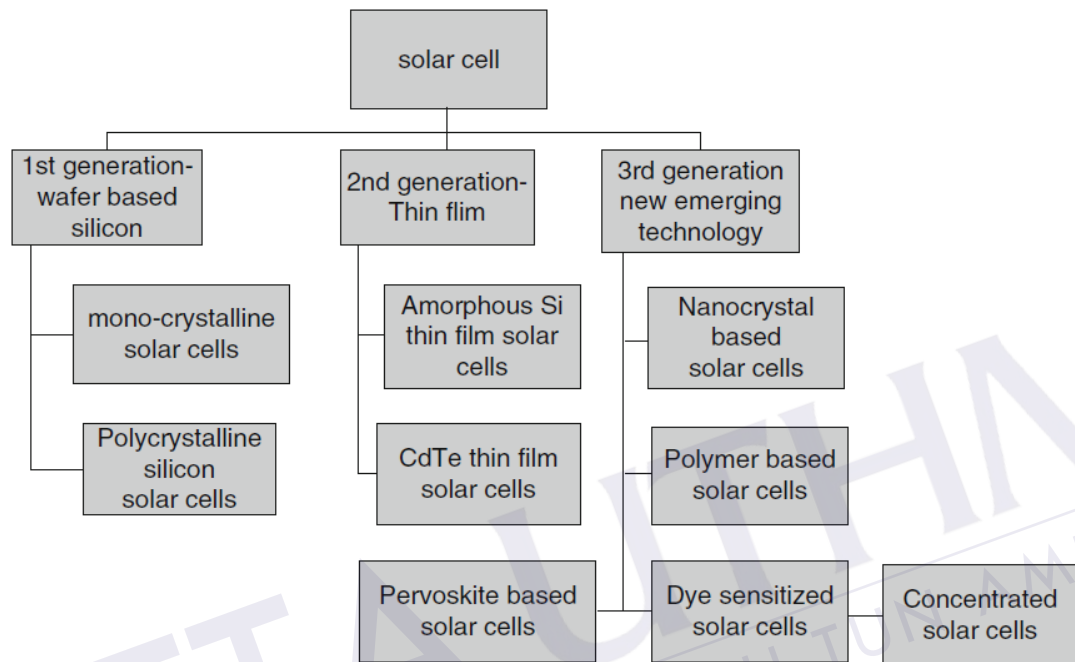


Figure 1.1: Generations of solar cells technology [5].

Dye-sensitized solar cells (DSSCs) is the third generation solar technology which provides effective charge separation that allows electricity to be generated even in low light condition. The first DSSCs was invented in 1991 based on artificial photosynthesis system to generate electricity [6]. Currently, DSSCs are still in the research phase to enhance its efficiency. The average efficiency of this new type of solar cells is 15% [7], [8]. Overall, DSSCs device manufacturing is considered as a low cost, simple and promising technique to provide high performance of electrical generation efficiency. DSSCs are currently in the testing stage to increase their performance. There are five components of a DSSCs. They are translucent fluoride-doped tin oxide (FTO) glass substrate, semiconductors material, dye sensitizer adsorber on the surface of the semiconductors, electrolytes, and counter electrodes (CE) [7].

REFERENCES

1. M. H. Bender, "Potential conservation of biomass in the production of synthetic organics," *Resources, Conservation and Recycling*, vol. 30, no. 1, pp. 49–58, 2000.
2. K. H. Solangi, M. R. Islam, R. Saidur, N. A. Rahim, and H. Fayaz, "A review on global solar energy policy," *Renewable and Sustainable Energy Reviews*, vol. 15, no. 4, pp. 2149–2163, 2011.
3. R. W. Miles, "Photovoltaic solar cells: Choice of materials and production methods," *Vacuum*, vol. 80, no. 10, pp. 1090–1097, 2006.
4. A. Jäger-Waldau, "Photovoltaics and renewable energies in Europe," *Renewable and Sustainable Energy Reviews*, vol. 11, no. 7, pp. 1414–1437, 2007.
5. C. M. Bhadra, P. G. Tharushi Perera, V. K. Truong, O. N. Ponamoreva, R. J. Crawford, and E. P. Ivanova, "Renewable bio-anodes for microbial fuel cells," *Handbook of Ecomaterials*, vol. 2, pp. 1167–1182, 2019.
6. B. and M. G. O'regan, "A low-cost, high-efficiency solar cell based on dye-sensitized," *Nature*, vol. 354, pp. 56–58, 1991.
7. M. K. Nazeeruddin, E. Baranoff, and M. Grätzel, "Dye-sensitized solar cells: A brief overview," *Solar Energy*, vol. 85, no. 6, pp. 1172–1178, 2011.
8. B. Li, L. Wang, B. Kang, P. Wang, and Y. Qiu, "Review of recent progress in solid-state dye-sensitized solar cells," *Solar Energy Materials and Solar Cells*, vol. 90, no. 5, pp. 549–573, 2006.
9. A. Goetzberger, J. Luther, and G. Willeke, "Solar cells: Past, present, future," *Solar Energy Materials and Solar Cells*, vol. 74, no. 1–4, pp. 1–11, 2002.
10. P. V. A. Baum, "The conversion of solar energy into electricity," *Solar Energy*, vol. 7, no. 4, pp. 180–187, 1963.

11. R. R. King, D. C. Law, K. M. Edmondson, C. M. Fetzer, G. S. Kinsey, H. Yoon, R. A. Sherif, and N. H. Karam, “40% efficient metamorphic GaInPGaInAsGe multijunction solar cells,” *Applied Physics Letters*, vol. 90, no. 18, pp. 90–93, 2007.
12. H. Gerischer, M. E. Michel-Beyerle, F. Rebentrost, and H. Tributsch, “Sensitization of charge injection into semiconductors with large band gap,” *Electrochimica Acta*, vol. 13, no. 6, pp. 1509–1515, 1968.
13. P. Wang, S. M. Zakeeruddin, R. Humphry-Baker, J. E. Moser, and M. Grätzel, “Molecular-Scale Interface Engineering of TiO₂ Nanocrystals: Improving the Efficiency and Stability of Dye-Sensitized Solar Cells,” *Advanced Materials*, vol. 15, no. 24, pp. 2101–2104, 2003.
14. M. Ye, X. Wen, M. Wang, J. Iocozzia, N. Zhang, C. Lin, and Z. Lin, “Recent advances in dye-sensitized solar cells: From photoanodes, sensitizers and electrolytes to counter electrodes,” *Materials Today*, vol. 18, no. 3, pp. 155–162, 2015.
15. A. Chiappone, F. Bella, J. R. Nair, G. Meligrana, R. Bongiovanni, and C. Gerbaldi, “Structure-Performance Correlation of Nanocellulose-Based Polymer Electrolytes for Efficient Quasi-solid DSSCs,” *ChemElectroChem*, vol. 1, no. 8, pp. 1350–1358, 2014.
16. E. I. Radeva, I. N. Martev, D. A. Dechev, N. Ivanov, V. N. Tsaneva, and Z. H. Barber, “Sensitivity to humidity of TiO₂ thin films obtained by reactive magnetron sputtering,” *Surface and Coatings Technology*, vol. 201, no. 6, pp. 2226–2229, 2006.
17. Y. O. Ken-ichiro Iuchi and A. F. Tetsu Tatsuma, “Cathode-Separated TiO₂ Photocatalysts Applicable to a Photochromic Device Responsive to Backside Illumination,” vol. 16, no. 7, pp. 10–12, 2004.
18. S. U. M. Khan, M. Al-Shahry, and W. B. Ingler, “Efficient photochemical water splitting by a chemically modified n-TiO₂,” *Science*, vol. 297, no. 5590, pp. 2243–2245, 2002.
19. X. Z. Li and F. B. Li, “Study of Au/Au³⁺-TiO₂ photocatalysts toward visible photooxidation for water and wastewater treatment,” *Environmental Science and Technology*, vol. 35, no. 11, pp. 2381–2387, 2001.
20. E. Reck and S. Seymour, “The effect of TiO₂ pigment on the performance of

- paratoluene sulphonic acid catalysed paint systems," *Journal of Chemical Information and Modeling*, vol. 53, no. 9, pp. 1689–1699, 2019.
21. J. J. Wu, G. R. Chen, H. H. Yang, C. H. Ku, and J. Y. Lai, "Effects of dye adsorption on the electron transport properties in ZnO-nanowire dye-sensitized solar cells," *Applied Physics Letters*, vol. 90, no. 21, pp. 2–5, 2007.
 22. Y. Wang, L. Zhang, K. Deng, X. Chen, and Z. Zou, "Low temperature synthesis and photocatalytic activity of rutile TiO₂ nanorod superstructures," *Journal of Physical Chemistry C*, vol. 111, no. 6, pp. 2709–2714, 2007.
 23. B. Liu and E. S. Aydil, "Growth of oriented single-crystalline rutile TiO₂ nanorods on transparent conducting substrates for dye-sensitized solar cells," *Journal of the American Chemical Society*, vol. 131, no. 11, pp. 3985–3990, 2009.
 24. K. Zhu, N. R. Neale, A. Miedaner, and A. J. Frank, "Enhanced charge-collection efficiencies and light scattering in dye-sensitized solar cells using oriented TiO₂ nanotubes arrays," *Nano Letters*, vol. 7, no. 1, pp. 69–74, 2007.
 25. B. Tan and Y. Wu, "Dye-sensitized solar cells based on anatase TiO₂ nanoparticle/nanowire composites," *Journal of Physical Chemistry B*, vol. 110, no. 32, pp. 15932–15938, 2006.
 26. A. T. Smith, A. M. LaChance, S. Zeng, B. Liu, and L. Sun, "Synthesis, properties, and applications of graphene oxide/reduced graphene oxide and their nanocomposites," *Nano Materials Science*, vol. 1, no. 1, pp. 31–47, 2019.
 27. N. A. F. Al-Rawashdeh, B. A. Albiss, and M. H. I. Yousef, "Graphene-Based Transparent Electrodes for Dye Sensitized Solar Cells," *IOP Conference Series: Materials Science and Engineering*, vol. 305, no. 1, 2018.
 28. Y. Chen, G. C. Egan, J. Wan, S. Zhu, R. J. Jacob, W. Zhou, J. Dai, Y. Wang, V. A. Danner, Y. Yao, K. Fu, Y. Wang, W. Bao, T. Li, M. R. Zachariah, and L. Hu, "Ultra-fast self-assembly and stabilization of reactive nanoparticles in reduced graphene oxide films," *Nature Communications*, vol. 7, pp. 1–9, 2016.
 29. E. Nouri, M. R. Mohammadi, and P. Lianos, "Impact of preparation method of TiO₂-RGO nanocomposite photoanodes on the performance of dye-sensitized solar cells," *Electrochimica Acta*, vol. 219, pp. 38–48, 2016.
 30. R. Zhao, Q. Geng, L. Chang, P. Wei, Y. Luo, X. Shi, A. M. Asiri, S. Lu, Z. Wang, and X. Sun, "Cu₃P nanoparticle-reduced graphene oxide hybrid: An

- efficient electrocatalyst to realize N₂-to-NH₃conversion under ambient conditions,” *Chemical Communications*, vol. 56, no. 65, pp. 9328–9331, 2020.
- 31. M. Szindler, W. Matysiak, M. Libera, P. Jarka, and M. Szindler, “Study of dye sensitized solar cells photoelectrodes consisting of nanostructures,” *Applied Surface Science*, vol. 491, pp. 807–813, 2019.
 - 32. V. Naresh and N. Lee, “A review on biosensors and recent development of nanostructured materials-enabled biosensors,” *Sensors (Switzerland)*, vol. 21, no. 4, pp. 1–35, 2021.
 - 33. M. Aftabuzzaman, C. Lu, and H. K. Kim, “Recent progress on nanostructured carbon-based counter/back electrodes for high-performance dye-sensitized and perovskite solar cells,” *Nanoscale*, vol. 12, no. 34, pp. 17590–17648, 2020.
 - 34. Y. Gu, T. Wang, Y. N. Dong, H. Zhang, D. Wu, and W. Chen, “Ferroelectric polyoxometalate-modified nano semiconductor TiO₂ for increasing electron lifetime and inhibiting electron recombination in dye-sensitized solar cells,” *Inorganic Chemistry Frontiers*, vol. 7, no. 17, pp. 3072–3080, 2020.
 - 35. F. Babar, U. Mehmood, H. Asghar, M. H. Mehdi, A. U. H. Khan, H. Khalid, N. ul Huda, and Z. Fatima, “Nanostructured photoanode materials and their deposition methods for efficient and economical third generation dye-sensitized solar cells: A comprehensive review,” *Renewable and Sustainable Energy Reviews*, vol. 129, no. May, 2020.
 - 36. A. Omar, M. S. Ali, and N. Abd Rahim, “Electron transport properties analysis of titanium dioxide dye-sensitized solar cells (TiO₂-DSSCs) based natural dyes using electrochemical impedance spectroscopy concept: A review,” *Solar Energy*, vol. 207, no. July, pp. 1088–1121, 2020.
 - 37. S. Ni, D. Wang, F. Guo, S. Jiao, Y. Zhang, B. Wang, L. Yuan, L. Zhang, L. Zhao, D. Wang, F. Guo, S. Jiao, Y. Zhang, J. Wang, B. Wang, L. Yuan, L. Zhang, and L. Zhao, “Accepted Manuscript,” 2018.
 - 38. G. A. M. Ali, M. M. Yusoff, H. Algarni, and K. F. Chong, “One-step electrosynthesis of MnO₂/rGO nanocomposite and its enhanced electrochemical performance,” *Ceramics International*, vol. 44, no. 7, pp. 7799–7807, 2018.
 - 39. M. Mohandoss, S. Sen Gupta, A. Nelleri, T. Pradeep, and S. M. Maliyekkal, “Solar mediated reduction of graphene oxide,” *RSC Advances*, vol. 7, no. 2, pp. 957–963, 2017.

40. M. Fathy, A. Gomaa, F. A. Taher, M. M. El-Fass, and A. E. H. B. Kashyout, "Optimizing the preparation parameters of GO and rGO for large-scale production," *Journal of Materials Science*, vol. 51, no. 12, pp. 5664–5675, 2016.
41. T. F. Emiru and D. W. Ayele, "Controlled synthesis, characterization and reduction of graphene oxide: A convenient method for large scale production," *Egyptian Journal of Basic and Applied Sciences*, vol. 4, no. 1, pp. 74–79, 2017.
42. K. Surana, S. Konwar, P. K. Singh, and B. Bhattacharya, "Utilizing reduced graphene oxide for achieving better efficient dye sensitized solar cells," *Journal of Alloys and Compounds*, vol. 788, pp. 672–676, 2019.
43. J. Chen, B. Yao, C. Li, and G. Shi, "An improved Hummers method for eco-friendly synthesis of graphene oxide," *Carbon*, vol. 64, no. 1, pp. 225–229, 2013.
44. W. Liu, K. Yin, F. He, Q. Ru, S. Zuo, and C. Yao, "A highly efficient reduced graphene oxide/SnO₂/TiO₂ composite as photoanode for photocathodic protection of 304 stainless steel," *Materials Research Bulletin*, vol. 113, no. December 2018, pp. 6–13, 2019.
45. F. I. Chowdhury, T. Blaine, and A. B. Gougam, "Optical transmission enhancement of fluorine doped tin oxide (FTO) on glass for thin film photovoltaic applications," *Energy Procedia*, vol. 42, pp. 660–669, 2013.
46. Z. and J. M. Jarzebski, "Physical properties of SnO₂ materials II. Electrical properties," 1976.
47. A. L. Dawar and J. C. Joshi, "Semiconducting transparent thin films: their properties and applications," *Journal of Materials Science*, vol. 19, no. 1, pp. 1–23, 1984.
48. L. Mahdavian, "Thermodynamic study of alcohol on SnO₂ (100)-based gas nano-sensor," *Physics and Chemistry of Liquids*, vol. 49, no. 5, pp. 626–638, 2011.
49. A. V. Moholkar, S. M. Pawar, K. Y. Rajpure, C. H. Bhosale, and J. H. Kim, "Effect of fluorine doping on highly transparent conductive spray deposited nanocrystalline tin oxide thin films," *Applied Surface Science*, vol. 255, no. 23, pp. 9358–9364, 2009.
50. B. Zhang, Y. Tian, J. X. Zhang, and W. Cai, "The role of oxygen vacancy in

- fluorine-doped SnO₂ films,” *Physica B: Condensed Matter*, vol. 406, no. 9, pp. 1822–1826, 2011.
51. K. Murakami, K. Nakajima, and S. Kaneko, “Initial growth of SnO₂ thin film on the glass substrate deposited by the spray pyrolysis technique,” *Thin Solid Films*, vol. 515, no. 24 SPEC. ISS., pp. 8632–8636, 2007.
 52. A. Fahmi, C. Minot, B. Silvi, and M. Causá, “Theoretical analysis of the structures of titanium dioxide crystals,” *Physical Review B*, vol. 47, no. 18, pp. 11717–11724, 1993.
 53. S. K. Simakov, “Nano- and micron-sized diamond genesis in nature: An overview,” *Geoscience Frontiers*, vol. 9, no. 6, pp. 1849–1858, 2018.
 54. X. D. and X. Liu, “Correlation between anatase-to-rutile transformation and grain growth in nanocrystalline titania powders,” *Science*, vol. 235, no. 4784, p. 9, 1998.
 55. D. Reyes-Coronado, G. Rodríguez-Gattorno, M. E. Espinosa-Pesqueira, C. Cab, R. De Coss, and G. Oskam, “Phase-pure TiO₂ nanoparticles: Anatase, brookite and rutile,” *Nanotechnology*, vol. 19, no. 14, 2008.
 56. J. Moellmann, S. Ehrlich, R. Tonner, and S. Grimme, “A DFT-D study of structural and energetic properties of TiO₂ modifications,” *Journal of Physics Condensed Matter*, vol. 24, no. 42, 2012.
 57. M. Xu, Y. Gao, E. M. Moreno, M. Kunst, M. Muhler, Y. Wang, H. Idriss, and C. Wöll, “Photocatalytic activity of bulk TiO₂ anatase and rutile single crystals using infrared absorption spectroscopy,” *Physical Review Letters*, vol. 106, no. 13, pp. 1–4, 2011.
 58. D. Cahen, G. Hodes, M. Grätzel, J. F. Guillemoles, and I. Riess, “Nature of Photovoltaic Action in Dye-Sensitized Solar Cells,” *Journal of Physical Chemistry B*, vol. 104, no. 9, pp. 2053–2059, 2000.
 59. Z. Lin, A. Orlov, R. M. Lambert, and M. C. Payne, “New insights into the origin of visible light photocatalytic activity of nitrogen-doped and oxygen-deficient anatase TiO₂,” *Journal of Physical Chemistry B*, vol. 109, no. 44, pp. 20948–20952, 2005.
 60. Y. Qiu, W. Chen, and S. Yang, “Double-layered photoanodes from variable-size anatase TiO₂ nanospindles: A candidate for high-efficiency dye-sensitized solar cells,” *Angewandte Chemie - International Edition*, vol. 49, no. 21, pp.

- 3675–3679, 2010.
61. D. A. H. Hanaor and C. C. Sorrell, “Review of the anatase to rutile phase transformation,” *Journal of Materials Science*, vol. 46, no. 4, pp. 855–874, 2011.
 62. M. Langlet, M. Burgos, C. Coutier, C. Jimenez, C. Morant, and M. Manso, “Low temperature preparation of high refractive index and mechanically resistant sol-gel TiO₂ films for multilayer antireflective coating applications,” *Journal of Sol-Gel Science and Technology*, vol. 22, no. 1–2, pp. 139–150, 2001.
 63. S. Das, S. Kar, and S. Chaudhuri, “Optical properties of SnO₂ nanoparticles and nanorods synthesized by solvothermal process,” *Journal of Applied Physics*, vol. 99, no. 11, 2006.
 64. H. Bin Wu, H. H. Hng, and X. W. D. Lou, “Direct synthesis of anatase TiO₂ nanowires with enhanced photocatalytic activity,” *Advanced Materials*, vol. 24, no. 19, pp. 2567–2571, 2012.
 65. R. C. Xie and J. K. Shang, “Morphological control in solvothermal synthesis of titanium oxide,” *Journal of Materials Science*, vol. 42, no. 16, pp. 6583–6589, 2007.
 66. H. G. Yang, G. Liu, S. Z. Qiao, C. H. Sun, Y. G. Jin, S. C. Smith, J. Zou, H. M. Cheng, and G. Q. Lu, “Solvothermal synthesis and photoreactivity of anatase TiO₂ nanosheets with dominant {001} facets,” *Journal of the American Chemical Society*, vol. 131, no. 11, pp. 4078–4083, 2009.
 67. H. Park, W. R. Kim, H. T. Jeong, J. J. Lee, H. G. Kim, and W. Y. Choi, “Fabrication of dye-sensitized solar cells by transplanting highly ordered TiO₂ nanotube arrays,” *Solar Energy Materials and Solar Cells*, vol. 95, no. 1, pp. 184–189, 2011.
 68. X. Liu, P. K. Chu, and C. Ding, “Surface modification of titanium, titanium alloys, and related materials for biomedical applications,” *Materials Science and Engineering R: Reports*, vol. 47, no. 3–4, pp. 49–121, 2004.
 69. M. T. SARODE, P. N. SHELKE, S. D. GUNJAL, Y. B. KHOLLAM, M. G. TAKWALE, S. R. JADKAR, B. B. KALE, K. C. MOHITE, and P. KOINKAR, “Effect of Annealing Temperature on Optical Properties of Titanium Dioxide Thin Films Prepared By Sol-Gel Method,” *International Journal of Modern*

- Physics: Conference Series*, vol. 06, pp. 13–18, 2012.
70. C.-P. Lin, H. Chen, A. Nakaruk, P. Koshy, and C. C. Sorrell, “Effect of Annealing Temperature on the Photocatalytic Activity of TiO₂ Thin Films,” *Energy Procedia*, vol. 34, pp. 627–636, 2013.
 71. M. M. Hasan, A. S. M. A. Haseeb, R. Saidur, and H. H. Masjuki, “Effects of annealing treatment on optical properties of anatase TiO₂ thin films,” *World Academy of Science, Engineering and Technology*, vol. 40, pp. 221–225, 2009.
 72. T. Peng, X. Xiao, F. Ren, J. Xu, X. Zhou, F. Mei, and C. Jiang, “Influence of annealing temperature on the properties of TiO₂ films annealed by ex situ and in situ TEM,” *Journal Wuhan University of Technology, Materials Science Edition*, vol. 27, no. 6, pp. 1014–1019, 2012.
 73. M. K. Ahmad, “Low temperature and normal pressure growth of rutile-phased TiO₂ nanorods/nanoflowers for DSC application prepared by hydrothermal method,” *Journal of Advanced Research in Physics*, vol. 3, no. 2, pp. 2011–2013, 2012.
 74. K. Byrappa and T. Adschari, “Hydrothermal technology for nanotechnology,” *Progress in Crystal Growth and Characterization of Materials*, vol. 53, no. 2, pp. 117–166, 2007.
 75. R. S. Mohar, S. Iwan, D. Djuhana, C. Imawan, A. Harmoko, and V. Fauzia, “Post-annealing effect on optical absorbance of hydrothermally grown zinc oxide nanorods,” *AIP Conference Proceedings*, vol. 1729, 2016.
 76. J. Zhang and L. Gao, “Synthesis and characterization of antimony-doped tin oxide (ATO) nanoparticles by a new hydrothermal method,” *Materials Chemistry and Physics*, vol. 87, no. 1, pp. 10–13, 2004.
 77. J. Gong, L. Luo, S. H. Yu, H. Qian, and L. Fei, “Synthesis of copper/cross-linked poly (vinyl alcohol) (PVA) nanocables via a simple hydrothermal route,” *Journal of Materials Chemistry*, vol. 16, no. 1, pp. 101–105, 2006.
 78. G. W. Morey and P. Niggli, “The hydrothermal formation of silicates, a review,” vol. 0, no. 1, p. 6, 1913.
 79. L. M. Dem’yanets and A. N. Lobachev, “Some Problems of Hydrothermal Crystallization,” *Crystallization Processes under Hydrothermal Conditions*, pp. 1–26, 1973.
 80. K. Byrappa, N. Keerthiraj, and S. M. Byrappa, *Crystals — Design and*

- Processing*. 2015.
81. G. Rajamanickam, S. Narendhiran, S. P. Muthu, S. Mukhopadhyay, and R. Perumalsamy, “Hydrothermally derived nanoporous titanium dioxide nanorods/nanoparticles and their influence in dye-sensitized solar cell as a photoanode,” *Chemical Physics Letters*, vol. 689, pp. 19–25, 2017.
 82. M. Marandi, Z. Goudarzi, and L. Moradi, “Synthesis of randomly directed inclined TiO₂ nanorods on the nanocrystalline TiO₂ layers and their optimized application in dye sensitized solar cells,” *Journal of Alloys and Compounds*, vol. 711, pp. 603–610, 2017.
 83. U. T. Pawar, S. A. Pawar, K. Jin-Hyeok, and P. S. Patil, “Dye sensitized solar cells based on hydrothermally grown TiO₂ nanostars over nanorods,” *Ceramics International*, 2016.
 84. S. M. Mokhtar, M. K. Ahmad, C. F. Soon, N. Nafarizal, A. B. Faridah, A. B. Suriani, M. H. Mamat, M. Shimomura, and K. Murakami, “Fabrication and characterization of rutile-phased titanium dioxide (TiO₂) nanorods array with various reaction times using one step hydrothermal method,” *Optik*, vol. 154, pp. 510–515, 2018.
 85. W. Li, J. Yang, Q. Jiang, Y. Luo, Y. Hou, S. Zhou, and Z. Zhou, “Bi-layer of nanorods and three-dimensional hierarchical structure of TiO₂ for high efficiency dye-sensitized solar cells,” *Journal of Power Sources*, vol. 284, pp. 428–434, 2015.
 86. K. H. Park and M. Dhayal, “Simultaneous growth of rutile TiO₂ as 1D/3D nanorod/nanoflower on FTO in one-step process enhances electrochemical response of photoanode in DSSC,” *Electrochemistry Communications*, vol. 49, pp. 47–50, 2015.
 87. Y. Jiang, M. Li, D. Song, X. Li, and Y. Yu, “A novel 3D structure composed of strings of hierarchical TiO₂ spheres formed on TiO₂ nanobelts with high photocatalytic properties,” *Journal of Solid State Chemistry*, vol. 211, pp. 90–94, 2014.
 88. M. B. Tahir, M. Rafique, M. S. Rafique, T. Nawaz, M. Rizwan, and M. Tanveer, “Photocatalytic nanomaterials for degradation of organic pollutants and heavy metals,” *Nanotechnology and Photocatalysis for Environmental Applications*, pp. 119–138, 2020.

89. L. F. Gorup, L. H. Amorin, E. R. Camargo, T. Sequinel, F. H. Cincotto, G. Biasotto, N. Ramesar, and F. de A. La Porta, “Methods for design and fabrication of nanosensors: the case of ZnO-based nanosensor,” *Nanosensors for Smart Cities*, pp. 9–30, 2020.
90. S. S. Taib, M. K. Ahmad, M. Z. A. Rahman, F. Mohamad, N. Nafarizal, C. F. Soon, A. S. Ameruddin, A. B. Faridah, M. Shimomura, and K. Murakami, “TiO₂ based dye-sensitized solar cell prepared by Spray Pyrolysis Deposition (SPD) technique,” *International Journal of Integrated Engineering*, vol. 10, no. 1, pp. 109–113, 2018.
91. O. A. Ileperuma, G. R. Asoka Kumara, H. S. Yang, and K. Murakami, “Quasi-solid electrolyte based on polyacrylonitrile for dye-sensitized solar cells,” *Journal of Photochemistry and Photobiology A: Chemistry*, vol. 217, no. 2–3, pp. 308–312, 2011.
92. G. R. A. Kumara, S. Kaneko, A. Konno, M. Okuya, K. Murakami, B. Onwona-agyeman, and K. Tennakone, “Large area dye-sensitized solar cells: Material aspects of fabrication,” *Progress in Photovoltaics: Research and Applications*, vol. 14, no. 7, pp. 643–651, 2006.
93. K. Kalyanasundaram and M. Gratzel, “Efficient dye-sensitized solar cells for direct conversion of sunlight to electricity.,,” *Material Matters (Milwaukee, WI, United States)*, vol. 4, no. 4, pp. 88–91, 2009.
94. U. Mehmood, S. U. Rahman, K. Harrabi, I. A. Hussein, and B. V. S. Reddy, “Recent advances in dye sensitized solar cells,” *Advances in Materials Science and Engineering*, vol. 2014, 2014.
95. M. Grätzel, “Conversion of sunlight to electric power by nanocrystalline dye-sensitized solar cells,” *Journal of Photochemistry and Photobiology A: Chemistry*, vol. 164, no. 1–3, pp. 3–14, 2004.
96. M. K. Nazeeruddin, R. Splivallo, P. Liska, P. Comte, and M. Grätzel, “A swift dye uptake procedure for dye sensitized solar cells,” *Chemical Communications*, vol. 12, pp. 1456–1457, 2003.
97. A. Mishra, M. K. R. Fischer, and P. Büuerle, “Metal-Free organic dyes for dye-Sensitized solar cells: From structure: Property relationships to design rules,” *Angewandte Chemie - International Edition*, vol. 48, no. 14, pp. 2474–2499, 2009.

98. H. Hug, M. Bader, P. Mair, and T. Glatzel, “Biophotovoltaics: Natural pigments in dye-sensitized solar cells,” *Applied Energy*, vol. 115, pp. 216–225, 2014.
99. K. Hara, Z. S. Wang, T. Sato, A. Furube, R. Katoh, H. Sugihara, Y. Dan-Oh, C. Kasada, A. Shinpo, and S. Suga, “Oligothiophene-containing coumarin dyes for efficient dye-sensitized solar cells,” *Journal of Physical Chemistry B*, vol. 109, no. 32, pp. 15476–15482, 2005.
100. K. Hara, Y. Tachibana, Y. Ohga, A. Shinpo, S. Suga, K. Sayama, H. Sugihara, and H. Arakawa, “Dye-sensitized nanocrystalline TiO₂ solar cells based on novel coumarin dyes,” *Solar Energy Materials and Solar Cells*, vol. 77, no. 1, pp. 89–103, 2003.
101. M. R. Narayan, “Review: Dye sensitized solar cells based on natural photosensitizers,” *Renewable and Sustainable Energy Reviews*, vol. 16, no. 1, pp. 208–215, 2012.
102. G. Calogero, G. Di Marco, S. Cazzanti, S. Caramori, R. Argazzi, A. Di Carlo, and C. A. Bignozzi, “Efficient dye-sensitized solar cells using red turnip and purple wild Sicilian prickly pear fruits,” *International Journal of Molecular Sciences*, vol. 11, no. 1, pp. 254–267, 2010.
103. J. Wu, Z. Lan, S. Hao, P. Li, J. Lin, M. Huang, L. Fang, and Y. Huang, “Progress on the electrolytes for dye-sensitized solar cells,” *Pure and Applied Chemistry*, vol. 80, no. 11, pp. 2241–2258, 2008.
104. F. T. Kong, S. Y. Dai, and K. J. Wang, “Review of recent progress in dye-sensitized solar cells,” *Advances in OptoElectronics*, vol. 2007, no. 1, pp. 1–13, 2007.
105. S. E. Koops, P. R. F. Barnes, B. C. O'Regan, and J. R. Durrant, “Kinetic competition in a coumarin dye-sensitized solar cell: Injection and recombination limitations upon device performance,” *Journal of Physical Chemistry C*, vol. 114, no. 17, pp. 8054–8061, 2010.
106. C. T. Yip, X. Liu, Y. Hou, W. Xie, J. He, S. Schlücker, D. Y. Lei, and H. Huang, “Strong competition between electromagnetic enhancement and surface-energy-transfer induced quenching in plasmonic dye-sensitized solar cells: A generic yet controllable effect,” *Nano Energy*, vol. 26, pp. 297–304, 2016.
107. Y. L. Lee, C. L. Chen, L. W. Chong, C. H. Chen, Y. F. Liu, and C. F. Chi, “A platinum counter electrode with high electrochemical activity and high

- transparency for dye-sensitized solar cells," *Electrochemistry Communications*, vol. 12, no. 11, pp. 1662–1665, 2010.
108. X. Fang, T. Ma, G. Guan, M. Akiyama, T. Kida, and E. Abe, "Effect of the thickness of the Pt film coated on a counter electrode on the performance of a dye-sensitized solar cell," *Journal of Electroanalytical Chemistry*, vol. 570, no. 2, pp. 257–263, 2004.
 109. C. Y. Lin, J. Y. Lin, C. C. Wan, and T. C. Wei, "High-performance and low platinum loading electrodeposited-Pt counter electrodes for dye-sensitized solar cells," *Electrochimica Acta*, vol. 56, no. 5, pp. 1941–1946, 2011.
 110. S. Ali and P. M. J. Elrod, "Biomimicry in Solar Energy Conversion with Natural Dye-Sensitized Nanocrystalline Photovoltaic Cells," in *Biochemistry*, 2007, pp. 1–22.
 111. S. S. Hegedus and A. Luque, "Status, Trends, Challenges and the Bright Future of Solar Electricity from Photovoltaics," in *Handbook of Photovoltaic Science and Engineering*, 2003, pp. 1–43.
 112. M. Grätzel, "Solar energy conversion by dye-sensitized photovoltaic cells," *Inorganic Chemistry*, vol. 44, no. 20, pp. 6841–6851, 2005.
 113. W. Guter, J. Schöne, S. P. Philipps, M. Steiner, G. Siefer, A. Wekkeli, E. Welser, E. Oliva, A. W. Bett, and F. Dimroth, "Current-matched triple-junction solar cell reaching 41.1% conversion efficiency under concentrated sunlight," *Applied Physics Letters*, vol. 94, no. 22, pp. 94–97, 2009.
 114. V. Baglio, M. Girolamo, V. Antonucci, and A. S. Aricò, "Influence of TiO₂ film thickness on the electrochemical behaviour of dye-sensitized solar cells," *International Journal of Electrochemical Science*, vol. 6, no. 8, pp. 3375–3384, 2011.
 115. S. James and R. Contractor, "Study on Nature-inspired Fractal Design-based Flexible Counter Electrodes for Dye-Sensitized Solar Cells Fabricated using Additive Manufacturing," *Scientific Reports*, vol. 8, no. 1, pp. 1–12, 2018.
 116. M. J. Jeng, Y. L. Wung, L. B. Chang, and L. Chow, "Particle size effects of TiO₂ layers on the solar efficiency of dye-sensitized solar cells," *International Journal of Photoenergy*, vol. 2013, 2013.
 117. K. Lee, R. Kirchgeorg, and P. Schmuki, "Role of transparent electrodes for high efficiency TiO₂ nanotube based dye-sensitized solar cells," *Journal of Physical*

- Chemistry C*, vol. 118, no. 30, pp. 16562–16566, 2014.
- 118. X. Liu and M. C. Hersam, “Interface Characterization and Control of 2D Materials and Heterostructures,” *Advanced Materials*, vol. 30, no. 39, pp. 1–34, 2018.
 - 119. F. Iskandar, U. Hikmah, E. Stavila, and A. H. Aimon, “Microwave-assisted reduction method under nitrogen atmosphere for synthesis and electrical conductivity improvement of reduced graphene oxide (rGO),” *RSC Advances*, vol. 7, no. 83, pp. 52391–52397, 2017.
 - 120. S. Basu and P. Bhattacharyya, “Recent developments on graphene and graphene oxide based solid state gas sensors,” *Sensors and Actuators, B: Chemical*, vol. 173, pp. 1–21, 2012.
 - 121. A. S. Lemine, M. M. Zagho, T. M. Altahtamouni, and N. Bensalah, “Graphene a promising electrode material for supercapacitors—A review,” *International Journal of Energy Research*, vol. 42, no. 14, pp. 4284–4300, 2018.
 - 122. A. A. Balandin, S. Ghosh, W. Bao, I. Calizo, D. Teweldebrhan, F. Miao, and C. N. Lau, “Superior thermal conductivity of single-layer graphene,” *Nano Letters*, vol. 8, no. 3, pp. 902–907, 2008.
 - 123. H. Zhang, D. Wang, J. Liu, H. Wei, F. Liu, J. Xu, S. Li, Z. Qin, J. Guo, R. Wang, H. Jia, J. Zhang, and Y. Liu, “Review on Thermal Conductivity of the Graphene Reinforced Resin Matrix Composites,” *IOP Conference Series: Materials Science and Engineering*, vol. 562, no. 1, 2019.
 - 124. I. V. G. and A. A. F. K. S. Novoselov, A. K. Geim, S. V. Morozov, D. Jiang, Y. Zhang, S. V. Dubonos, “Electric Field Effect in Atomically Thin Carbon Films,” vol. 306, no. 5696, pp. 666–669, 2016.
 - 125. C. Huang, S. Gupta, C. Lo, N. Tai, and S. Gupta, “Highly transparent and excellent electromagnetic interference shielding hybrid films composed of sliver-grid/(silver nanowires and reduced graphene oxide),” *Materials Letters*, vol. 253, pp. 152–155, 2019.
 - 126. R. R. Nair, P. Blake, A. N. Grigorenko, K. S. Novoselov, T. J. Booth, T. Stauber, N. M. R. Peres, and A. K. Geim, “Fine structure constant defines visual transparency of graphene,” *Science*, vol. 320, no. 5881, p. 1308, 2008.
 - 127. M. D. Stoller, S. Park, Y. Zhu, J. An, and R. S. Ruoff, “Graphene-Based Ultracapacitors,” *Nano Letters*, vol. 8, no. 10, pp. 3498–3502, 2008.

128. M. F. Y. M. Hanappi, M. Deraman, M. Suleman, M. A. R. Othman, N. H. Basri, N. S. M. Nor, E. Hamdan, N. E. S. Sazali, and N. S. M. Tajuddin, "Preparation and characterization of graphene/turbostratic carbon derived from chitosan film for supercapacitor electrodes," *AIP Conference Proceedings*, vol. 1940, no. 1, pp. 1–8, 2018.
129. C. Lee, X. Wei, J. W. Kysar, and J. Hone, "Measurement of the elastic properties and intrinsic strength of monolayer graphene," *Science*, vol. 321, no. 5887, pp. 385–388, 2008.
130. K. M. Wibowo, M. Z. Sahdan, N. I. Ramli, A. Muslihati, N. Rosni, V. H. Tsen, H. Saim, S. A. Ahmad, Y. Sari, and Z. Mansor, "Detection of Escherichia Coli Bacteria in Wastewater by using Graphene as a Sensing Material," *Journal of Physics: Conference Series*, vol. 995, no. 1, 2018.
131. M. Kalbacova, A. Broz, J. Kong, and M. Kalbac, "Graphene substrates promote adherence of human osteoblasts and mesenchymal stromal cells," *Carbon*, vol. 48, no. 15, pp. 4323–4329, 2010.
132. S. S. Varghese, S. Lonkar, K. K. Singh, S. Swaminathan, and A. Abdala, "Recent advances in graphene based gas sensors," *Sensors and Actuators, B: Chemical*, vol. 218, pp. 160–183, 2015.
133. F. Liu, X. Chu, Y. Dong, W. Zhang, W. Sun, and L. Shen, "Acetone gas sensors based on graphene-ZnFe₂O₄ composite prepared by solvothermal method," *Sensors and Actuators, B: Chemical*, vol. 188, pp. 469–474, 2013.
134. K. Tadyszak, J. K. Wychowaniec, and J. Litowczenco, "Biomedical applications of graphene-based structures," *Nanomaterials*, vol. 8, no. 11, pp. 1–20, 2018.
135. G. S. Selopal, R. Milan, L. Ortolani, V. Morandi, R. Rizzoli, G. Sberveglieri, G. P. Veronese, A. Vomiero, and I. Concina, "Graphene as transparent front contact for dye sensitized solar cells," *Solar Energy Materials and Solar Cells*, vol. 135, pp. 99–105, 2015.
136. C. D. Reddy, S. Rajendran, and K. M. Liew, "Equilibrium configuration and continuum elastic properties of finite sized graphene," *Nanotechnology*, vol. 17, no. 3, pp. 864–870, 2006.
137. S. Sajjad, S. A. Khan Leghari, and A. Iqbal, "Study of Graphene Oxide Structural Features for Catalytic, Antibacterial, Gas Sensing, and Metals

- Decontamination Environmental Applications," *ACS Applied Materials and Interfaces*, vol. 9, no. 50, pp. 43393–43414, 2017.
- 138. U. A. Kanta, V. Thongpool, W. Sangkun, N. Wongyao, and J. Wootthikanokkhan, "Preparations, characterizations, and a comparative study on photovoltaic performance of two different types of graphene/TiO₂ nanocomposites photoelectrodes," *Journal of Nanomaterials*, vol. 2017, pp. 1–13, 2017.
 - 139. D. Kumaresan, S. Jothi, J. D. Mcgettrick, T. M. Watson, D. Kumaresan, S. Jothi, J. D. Mcgettrick, T. M. Watson, and A. Surface, "Reduced graphene oxide wrapped hierarchical TiO₂ nanorod composites for improved charge collection efficiency and carrier lifetime in dye sensitized solar cells," *Applied Surface Science*, vol. 428, pp. 439–447, 2018.
 - 140. H. Cai, J. Li, X. Xu, H. Tang, J. Luo, K. Binnemans, D. E. De Vos, J. Li, X. Xu, H. Tang, J. Luo, K. Binnemans, J. Fransaer, and D. E. De Vos, "Nanostructured composites of one-dimensional TiO₂ and reduced graphene oxide for efficient dye-sensitized solar cells," *Journal of Alloys and Compounds*, vol. 697, pp. 132–137, 2016.
 - 141. A. B. Suriani, Muqoyyanah, A. Mohamed, M. H. Mamat, M. H. D. Othman, M. K. Ahmad, H. P. S. Abdul Khalil, P. Marwoto, and M. D. Birowosuto, "Titanium dioxide/agglomerated-free reduced graphene oxide hybrid photoanode film for dye-sensitized solar cells photovoltaic performance improvement," *Nano-Structures and Nano-Objects*, vol. 18, pp. 1–14, 2019.
 - 142. M. K. Ahmad, C. F. Soon, N. Nafarizal, A. B. Suriani, A. Mohamed, M. H. Mamat, M. F. Malek, M. Shimomura, and K. Murakami, "Effect of heat treatment to the rutile based dye sensitized solar cell," *Optik*, vol. 127, no. 8, pp. 4076–4079, 2016.
 - 143. B. Viswanathan and K. J. A. Raj, "Effect of surface area, pore volume and particle size of P25 titania on the phase transformation of anatase to rutile," *Indian Journal of Chemistry - Section A Inorganic, Physical, Theoretical and Analytical Chemistry*, vol. 48, no. 10, pp. 1378–1382, 2009.
 - 144. J. Zhang, P. Zhou, J. Liu, and J. Yu, "New understanding of the difference of photocatalytic activity among anatase, rutile and brookite TiO₂," *Physical Chemistry Chemical Physics*, vol. 16, no. 38, pp. 20382–20386, 2014.

145. P. Benjwal, B. De, and K. K. Kar, “1-D and 2-D morphology of metal cation co-doped (Zn, Mn) TiO₂ and investigation of their photocatalytic activity,” *Applied Surface Science*, vol. 427, pp. 262–272, 2018.
146. A. B. Suriani, A. Mohamed, N. Hashim, M. S. Rosmi, M. H. Mamat, M. F. Malek, M. J. Salifairus, and H. P. S. A. Khalil, “Reduced graphene oxide/platinum hybrid counter electrode assisted by custom-made triple-tail surfactant and zinc oxide/titanium dioxide bilayer nanocomposite photoanode for enhancement of DSSCs photovoltaic performance,” *Optik*, vol. 161, pp. 70–83, 2018.
147. A. B. Suriani, M. D. Nurhafizah, A. Mohamed, M. H. Mamat, M. F. Malek, M. K. Ahmad, A. Pandikumar, and N. M. Huang, “Enhanced photovoltaic performance using reduced graphene oxide assisted by triple-tail surfactant as an efficient and low-cost counter electrode for dye-sensitized solar cells,” *Optik*, vol. 139, pp. 291–298, 2017.
148. F. I. M. Fazli, M. K. Ahmad, C. F. Soon, N. Nafarizal, A. B. Suriani, A. Mohamed, M. H. Mamat, M. F. Malek, M. Shimomura, and K. Murakami, “Dye-sensitized solar Cell using pure anatase TiO₂ annealed at different temperatures,” *Optik*, vol. 140, pp. 1063–1068, 2017.
149. F. W. Low, C. W. Lai, S. Bee, and A. Hamid, “Facile Synthesis of High Quality Graphene Oxide from Graphite Flakes Using Improved Hummer ’ s Technique,” *Journal of Nanoscience and NanotechnologyNanotechnology*, vol. 15, no. 1, pp. 1–5, 2015.
150. Y. S. Lim, Y. P. Tan, H. N. Lim, W. T. Tan, M. A. Mahnaz, Z. A. Talib, N. M. Huang, A. Kassim, and M. A. Yarmo, “Polypyrrole/graphene composite films synthesized via potentiostatic deposition,” *Journal of Applied Polymer Science*, vol. 128, no. 1, pp. 224–229, 2013.
151. M. Jithin, K. Saravanakumar, V. Ganesan, V. R. Reddy, P. M. Razad, M. M. Patidar, K. Jeyadheepan, G. Marimuthu, V. R. Sreelakshmi, and K. Mahalakshmi, “Growth, mechanism and properties of TiO₂nanorods embedded nanopillar: Evidence of lattice orientation effect,” *Superlattices and Microstructures*, vol. 109, pp. 145–153, 2017.
152. J. Lin, Y. U. Heo, A. Nattestad, Z. Sun, L. Wang, J. H. Kim, and S. X. Dou, “3D hierarchical rutile TiO₂ and metal-free organic sensitizer producing dye-

- sensitized solar cells 8.6% conversion efficiency," *Scientific Reports*, vol. 4, pp. 1–8, 2014.
153. H. Z. Asl and S. M. Rozati, "High-quality spray-deposited fluorine-doped tin oxide: effect of film thickness on structural, morphological, electrical, and optical properties," *Applied Physics A: Materials Science and Processing*, vol. 125, no. 10, pp. 1–8, 2019.
154. L. H. Lalasari, T. Arini, L. Andriyah, F. Firdiyono, and A. H. Yuwono, "Electrical, optical and structural properties of FTO thin films fabricated by spray ultrasonic nebulizer technique from SnCl_4 precursor," *AIP Conference Proceedings*, vol. 1964, no. May 2018, 2018.
155. H. Sutiono, A. M. Tripathi, H. M. Chen, C. H. Chen, W. N. Su, L. Y. Chen, H. Dai, and B. J. Hwang, "Facile synthesis of [101]-oriented rutile TiO_2 nanorod array on FTO substrate with a tunable anatase-rutile heterojunction for efficient solar water splitting," *ACS Sustainable Chemistry and Engineering*, vol. 4, no. 11, pp. 5963–5971, 2016.
156. X. Kang, S. Liu, Z. Dai, Y. He, X. Song, and Z. Tan, "Titanium dioxide: From engineering to applications," *Catalysts*, vol. 9, no. 2, pp. 1–32, 2019.
157. M. Barthomeuf, X. Castel, L. Le Gendre, J. Louis, M. Denis, and C. Pissavini, "Effect of Titanium Dioxide Film Thickness on Photocatalytic and Bactericidal Activities Against *Listeria monocytogenes*," *Photochemistry and Photobiology*, vol. 95, no. 4, pp. 1035–1044, 2019.
158. A. Talib, M. K. Ahmad, N. Nafarizal, F. Mohamad, C. F. Soon, A. B. Suriani, M. H. Mamat, K. Murakami, and M. Shimomura, "Performance of dye-sensitized solar cell using size-controlled synthesis of TiO_2 nanostructure," *International Journal of Integrated Engineering*, vol. 12, no. 2, pp. 106–114, 2020.
159. M. Imran, S. Riaz, and S. Naseem, "Synthesis and Characterization of Titania Nanoparticles by Sol-gel Technique," *Materials Today: Proceedings*, vol. 2, no. 10, pp. 5455–5461, 2015.
160. M. K. Ahmad, S. M. Mokhtar, C. F. Soon, N. Nafarizal, A. B. Suriani, A. Mohamed, M. H. Mamat, M. F. Malek, M. Shimomura, and K. Murakami, "Raman investigation of rutile-phased TiO_2 nanorods/nanoflowers with various reaction times using one step hydrothermal method," *Journal of Materials*

- Science: Materials in Electronics*, vol. 27, no. 8, pp. 7920–7926, 2016.
161. S. Shalini, N. Prabavathy, R. Balasundaraprabhu, T. S. Kumar, D. Velauthapillai, P. Balraju, and S. Prasanna, “Studies on DSSC encompassing flower shaped assembly of Na-doped TiO₂ nanorods sensitized with extract from petals of *Kigelia Africana*,” *Optik*, vol. 155, pp. 334–343, 2018.
 162. V. V. Burungale, V. V. Satale, A. J. More, K. K. K. Sharma, A. S. Kamble, J. H. Kim, and P. S. Patil, “Studies on effect of temperature on synthesis of hierarchical TiO₂ nanostructures by surfactant free single step hydrothermal route and its photoelectrochemical characterizations,” *Journal of Colloid and Interface Science*, vol. 470, pp. 108–116, 2016.
 163. G. C. Collazzo, S. L. Jahn, N. L. V. Carreño, and E. L. Foletto, “Temperature and reaction time effects on the structural properties of titanium dioxide nanopowders obtained via the hydrothermal method,” *Brazilian Journal of Chemical Engineering*, vol. 28, no. 2, pp. 265–272, 2011.
 164. S. Shamsudin, M. K. Ahmad, N. Nafarizal, C. F. Soon, R. A. Rahim, D. A. L. Alakendram, M. Shimomura, and K. Murakami, “Fabrication of TiO₂ nanoflowers powder with various concentration of CTAB,” *International Journal of Integrated Engineering*, vol. 12, no. 2, pp. 197–205, 2020.
 165. S. B. Wategaonkar, R. P. Pawar, V. G. Parale, D. P. Nade, B. M. Sargar, and R. K. Mane, “Synthesis of rutile TiO₂ nanostructures by single step hydrothermal route and its characterization,” *Materials Today: Proceedings*, vol. 23, pp. 444–451, 2020.
 166. S. Livraghi, A. M. Czoska, M. C. Paganini, and E. Giamello, “Preparation and spectroscopic characterization of visible light sensitized N doped TiO₂ (rutile),” *Journal of Solid State Chemistry*, vol. 182, no. 1, pp. 160–164, 2009.
 167. M. R. D. Khaki, M. S. Shafeeyan, A. A. A. Raman, and W. M. A. W. Daud, “Application of doped photocatalysts for organic pollutant degradation - A review,” *Journal of Environmental Management*, vol. 198, pp. 78–94, 2017.
 168. N. Jiang, Y. Du, S. Liu, M. Du, Y. Feng, and Y. Liu, “Facile preparation of flake-like blue TiO₂ nanorod arrays for efficient visible light photocatalyst,” *Ceramics International*, no. January, pp. 1–7, 2019.
 169. F. W. Low, C. W. Lai, and S. B. A. Hamid, “One-step hydrothermal synthesis of titanium dioxide decorated on reduced graphene oxide for dye-sensitised

- solar cells application," *International Journal of Nanotechnology*, vol. 15, no. 1/2/3, p. 78, 2018.
170. H. Zhang, Y. Lv, C. Yang, H. Chen, and X. Zhou, "One-Step Hydrothermal Fabrication of TiO₂/Reduced Graphene Oxide for High-Efficiency Dye-Sensitized Solar Cells," *Journal of Electronic Materials*, vol. 47, no. 2, pp. 1630–1637, 2018.
171. S. Z. Siddick, C. W. Lai, J. C. Juan, and S. B. Hamid, "Reduced Graphene Oxide - Titania Nanocomposite Film for Improving Dye-Sensitized Solar Cell (DSSCs) Performance," *Current Nanoscience*, vol. 13, no. 5, 2017.
172. Y. Zhang, W. Wu, K. Zhang, C. Liu, A. Yu, M. Peng, and J. Zhai, "Raman study of 2D anatase TiO₂ nanosheets," *Phys. Chem. Chem. Phys.*, vol. 18, no. 47, pp. 32178–32184, 2016.
173. R. Hazem, M. Izerrouken, A. Cheraitia, and A. Djehlane, "Raman study of ion beam irradiation damage on nanostructured TiO₂ thin film," *Nuclear Instruments and Methods in Physics Research, Section B: Beam Interactions with Materials and Atoms*, vol. 444, no. October 2018, pp. 62–67, 2019.
174. M. Tortello, S. Colonna, M. Bernal, J. Gomez, M. Pavese, C. Novara, F. Giorgis, M. Maggio, G. Guerra, G. Saracco, R. S. Gonnelli, and A. Fina, "Effect of thermal annealing on the heat transfer properties of reduced graphite oxide flakes: A nanoscale characterization via scanning thermal microscopy," *Carbon*, vol. 109, pp. 390–401, 2016.
175. Y. J. Xu, Y. Zhuang, and X. Fu, "New insight for enhanced photocatalytic activity of TiO₂ by doping carbon nanotubes: A case study on degradation of benzene and methyl orange," *Journal of Physical Chemistry C*, vol. 114, no. 6, pp. 2669–2676, 2010.
176. F. I. M. Fazli, N. Nayan, M. K. Ahmad, M. L. M. Napi, N. K. A. Hamed, and N. S. Khalid, "Effect of annealing temperatures on TiO₂ thin films prepared by spray pyrolysis deposition method," *Sains Malaysiana*, vol. 45, no. 8, pp. 1197–1200, 2016.
177. V. Madurai Ramakrishnan, N. Muthukumarasamy, S. Pitchaiya, S. Agilan, A. Pugazhendhi, and D. Velauthapillai, "UV-aided graphene oxide reduction by TiO₂ towards TiO₂/reduced graphene oxide composites for dye-sensitized solar cells," *International Journal of Energy Research*, vol. 45, no. 12, pp. 17220–

- 17232, Oct. 2021.
178. K. A. Kumar, K. Subalakshmi, and J. Senthilselvan, "Effect of co-sensitization in solar exfoliated TiO₂ functionalized rGO photoanode for dye-sensitized solar cell applications," *Materials Science in Semiconductor Processing*, vol. 96, no. January, pp. 104–115, 2019.
 179. J. Ma, W. Ren, J. Zhao, and H. Yang, "Growth of TiO₂ nanoflowers photoanode for dye-sensitized solar cells," *Journal of Alloys and Compounds*, vol. 692, pp. 1004–1009, 2017.
 180. L. Gomathi Devi and M. Srinivas, "Hydrothermal synthesis of reduced graphene oxide-CoFe₂O₄ heteroarchitecture for high visible light photocatalytic activity: Exploration of efficiency, stability and mechanistic pathways," *Journal of Environmental Chemical Engineering*, vol. 5, no. 4, pp. 3243–3255, 2017.
 181. M. A. Agam, N. N. Awal, S. A. Hassan, J. A. Yabagi, M. Q. Hamzah, and A. Talib, "Energy band gap investigation of polystyrene copper oxide nanocomposites bombarded with laser," *Journal of Advanced Research in Fluid Mechanics and Thermal Sciences*, vol. 66, no. 2, pp. 125–135, 2020.
 182. A. Omar, M. S. Fakir, K. S. Hamdan, N. H. Rased, and N. A. Rahim, "Photovoltaic performances and lifetime analysis of TiO₂/rGO DSSCs sensitized with Roselle and N719 dyes," *IOP Conference Series: Materials Science and Engineering*, vol. 1127, no. 1, p. 012041, 2021.
 183. M. Y. A. Rahman, A. S. Sulaiman, A. A. Umar, and M. M. Salleh, "Dye-sensitized solar cell (DSSC) utilizing reduced graphene oxide (RGO) films counter electrode: effect of graphene oxide (GO) content," *Journal of Materials Science: Materials in Electronics*, pp. 1674–1678, 2017.
 184. T. Supasai, N. Henjongchom, I. M. Tang, F. Deng, and N. Rujisamphan, "Compact nanostructured TiO₂ deposited by aerosol spray pyrolysis for the hole-blocking layer in a CH₃NH₃PbI₃ perovskite solar cell," *Solar Energy*, vol. 136, pp. 515–524, 2016.
 185. A. B. Suriani, N. Nafarizal, M. K. Ahmad, M. Shimomura, M. H. Mamat, A. B. Faridah, C. F. Soon, K. Murakami, and S. M. Mokhtar, "Fabrication and characterization of rutile-phased titanium dioxide (TiO₂) nanorods array with various reaction times using one step hydrothermal method," *Optik*, vol. 154,

- pp. 510–515, 2017.
186. F. W. Low, C. W. Lai, K. M. Lee, and J. C. Juan, “Enhance of TiO₂ dopants incorporated reduced graphene oxide via RF magnetron sputtering for efficient dye-sensitised solar cells,” *Rare Metals*, vol. 37, no. 11, pp. 919–928, 2018.

